DOI: 10.1002/cmdc.200800434

Adenosine A_{2A} Receptor Antagonists: New 8-Substituted 9-Ethyladenines as Tools for in vivo Rat Models of Parkinson's Disease

Rosaria Volpini,*[a] Diego Dal Ben,[a] Catia Lambertucci,[a] Gabriella Marucci,[a] Ram Chandra Mishra,[a] Anna Teresa Ramadori,[a] Karl-Norbert Klotz,[b] Maria Letizia Trincavelli,[c] Claudia Martini,[c] and Gloria Cristalli[a]

Clinical evidence has demonstrated that $AA_{2A}R$ antagonists could be an alternative approach to the treatment of Parkinson's disease. Recently, three 9-ethyladenine derivatives bearing a bromine atom, an ethoxy group, and a furyl ring, respectively, in the 8-position have been reported to ameliorate motor deficits in rat Parkinson's disease models, suggesting a potential therapeutic role for these compounds. Starting from these observations, a new series of 9-ethyladenine derivatives, bearing different substituents such as halogens, alkoxy groups, aromatic and heteroaromatic rings in the 8-position, were synthesized. Radioligand binding assays demonstrated that some of the new compounds bind rat $AA_{2A}R$ with higher affinity than the previously reported congeners and that there is a good correlation between binding to rat and human receptors. Hence, the new molecules could represent new tools suitable for the in vivo studies in rat models of Parkinson's disease. Finally, a molecular docking analysis of the compounds was performed using a homology model of rat $AA_{2A}R$, built using the human crystal structure as the template, and results are in agreement with the binding data.

Introduction

Adenosine, a naturally occurring nucleoside, is involved in a wide variety of physiological and pathophysiological processes.[1] Some of its physiological actions include effects on heart rate and atrial contractility, vascular smooth muscle tone, release of neurotransmitters, platelet function, lipolysis, renal function and white blood cell function.[2] Adenosine mediates these effects through the activation of at least four human receptors (P1) belonging to the superfamily of G-protein-coupled receptors, which have been recently cloned[3] and classified as A_1, A_{2A}, A_{2B}, and A_3.[4,5] The subtypes are classified on the basis of coupling to second messengers, as well as pharmacological profiles for agonists and antagonists. In fact, adenosine A_1 and A_3 receptors (AA_1R and AA_3R, respectively) are linked to inhibition of adenylyl cyclase, while A_{2A} and A_{2B} subtypes ($AA_{2A}R$ and $AA_{2B}R$, respectively) are linked to stimulation of the same enzyme.[6]

The prototypical adenosine receptor (AR) antagonists are naturally occurring methylxanthines which have been extensively modified for increased potency and selectivity toward specific AR subtypes.[7–9] However, only a few xanthine antagonists, such as caffeine and theophylline, have been approved as drugs for their CNS-stimulating, diuretic, and bronchodilating effects.[9,10] Hence, many efforts in recent decades have been directed toward the synthesis and development of new AR antagonists endowed with high affinity and subtype selectivity. These antagonists include different classes of nitrogen polyheterocyclic systems[11] such as pyrazolo[1,5-*a*]pyridines, pyrazolo[4,3-*e*][1,2,4]triazolo[1,5-*c*]pyrimidines, pyrrolopyrimidines, 1,4-dihydropyridines, pyridines, and aminopyrimidines.[12]

Other AR antagonists, the structure of which directly correlate to the natural ligand adenosine, exhibit adenine core substitutions. Many publications have demonstrated that introduction of different substituents in the 2-, 8-, and 9-position of adenine result in high-affinity antagonists with distinct receptor selectivity profiles.[13–17] Hence, substituted adenine derivatives, prepared as hypoglycemic agents, were found to possess high potency for the $AA_{2B}R$ subtype,[18] whereas novel *N*6-cyclopentyladenine derivatives were characterized as neutral antagonists endowed with high affinity for AA_1R.[19] In contrast, 2-phenylaminoadenines bearing a variety of cycloalkyl rings at the N6 position were found to possess high affinity for AA_3R.[20]

Recent clinical evidence has demonstrated that $AA_{2A}R$ antagonists effectively decrease motor impairment in Parkinsonian patients who have low risk of dyskinesia, potentially providing an alternative approach for the treatment of Parkinson's disease.[21–23] Accordingly, we reported that three 9-ethyladenine (**1**) derivatives, each bearing a bromine, ethoxy group, or furyl

[a] *Prof. R. Volpini, Dr. D. Dal Ben, Dr. C. Lambertucci, Prof. Dr. G. Marucci, Dr. R. C. Mishra, Dr. A. T. Ramadori, Prof. G. Cristalli*
Dipartimento di Scienze Chimiche, Università di Camerino
via S. Agostino 1, 62032 Camerino (MC) (Italy)
Fax: (+39) 0737-402295
E-mail: rosaria.volpini@unicam.it

[b] *Prof. K.-N. Klotz*
Institut für Pharmakologie und Toxikologie
Versbacher Str. 9, 97078 Würzburg (Germany)

[c] *Dr. M. L. Trincavelli, Prof. C. Martini*
Dipartimento di Psichiatria, Neurobiologia, Farmacologia e Biotecnologie
Università di Pisa, Via Bonanno Pisano 6, 56010 Pisa (Italy)

ring at the 8-position (compounds **2**, **7**, and **11**, respectively), bind human $AA_{2A}R$ with nanomolar affinity[14,24,25] and ameliorate motor deficits in rat models of Parkinson's disease, providing further evidence of a possible therapeutic role for these compounds.[26]

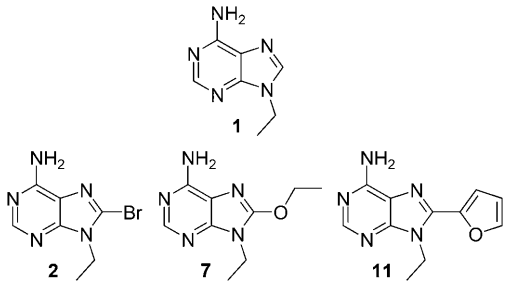

Beginning with these observations, we aimed to produce compounds endowed with improved affinity and selectivity at rat and human $AA_{2A}R$. A series of novel purine derivatives was prepared by introducing various substituents at the 8-position of 9-ethyladenine. Taking into account the structures of aforementioned $AA_{2A}R$ antagonists **2**, **7**, and **11**, our compounds were specifically designed with halogens, alkoxy groups, aromatic, and heteroaromatic rings at this position. Other 8-position derivatives included small substituents with a variety of electronic properties, such as methyl, trifluoromethyl, and hydroxy groups.

These compounds, together with **2**, **7**, **11**, **9**, and **20**, the activities of which at human ARs have already been reported,[14,24,25] were screened using radioligand binding assays in rat ARs. The importance of characterizing the affinity of these molecules for rat membrane receptors is based on future plans to test in in vivo rat models of Parkinson's disease, although they are intended for pharmacological use in humans. Some of the novel compounds were also tested in binding assays with human ARs for comparison with rat AR binding data. Finally, a molecular docking analysis of the new 9-ethyladenine derivatives was performed using a homology model of rat $AA_{2A}R$, built using the human $AA_{2A}R$ crystal structure as a template.[27] This analysis was carried out with the aim at finding a possible rationalization of the different binding affinities of the molecules for the rat $AA_{2A}R$, as well as enabling further optimization of this class of adenosine antagonists.

Results and Discussion

Chemistry

The 8-halogen derivatives **2**–**4** were synthesized from 9-ethyladenine (**1**), which was prepared as previously reported.[13,14] Reaction of **1** with *N*-bromosuccinimide (NBS) or *N*-chlorosuccinimide (NCS) was carried out in dry DMF at room temperature for 20 h to yield the corresponding 8-bromo- and 8-chloro-9-ethyladenine (**2**[10] and **3**, respectively). 9-ethyl-8-iodo-9*H*-adenine (**4**) was obtained by treating **1** with lithium diisopropylamide (LDA) and then I_2 in anhydrous THF (Scheme 1). 8-hydroxy-9-ethyladenine (**5**) was synthesized from **2**, following reaction with 98% HCO_2H at reflux, whereas the 9-ethyl-8-alkoxy adenine derivatives **6**–**10** were obtained by allowing **2** to react with the corresponding alcohols, using catalytic sodium hydroxide (Scheme 2). Synthesis of **11** and **12** was accomplished beginning with **2**, which was reacted in anhydrous THF with the 2-tributylstannyl derivatives of furan and thiophene, respectively, using catalytic bis(triphenylphosphine)palladium dichloride. Reduction of **11** using PdO in H_2 atmosphere under acidic conditions yielded **13** (Scheme 2). For the synthesis of **14**, compound **2** was added to sodium trifluoroacetate and copper iodide under N_2 atmosphere at 80 °C for 2.5 h. The C8 methyl- and phenyl-substituted compounds were synthesized using a different method involving a cyclization to yield the purine structure (Scheme 3).

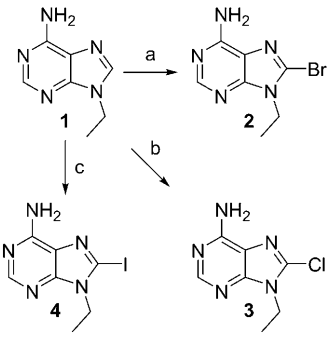

Scheme 1. Reagents and conditions: a) NBS, DMF; b) NCS, DMF; c) LDA/I_2, THF.

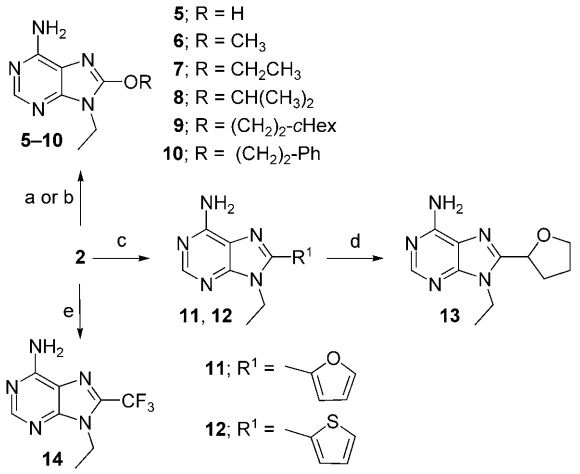

Scheme 2. Reagents and conditions: a) HCOOH; b) NaOH, ROH; c) (nBu)$_3$Sn-R^1, $(Ph_3P)_2PdCl_2$, THF; d) H_2/PdO; e) CF_3COONa.

Ethylamine and 5-amino-4,6-dichloropyrimidine (**15**) were combined in a sealed bomb at 150 °C for 27 h, to obtain 5-amino-4-chloro-6-ethylaminopyrimidine (**16**), which had been previously synthesized using a different procedure.[28] Reaction of **16** with triethylorthoacetate (TEOA) or triethylorthobenzoate (TEOB) at room temperature for 12 h, using catalytic methanesulfonic acid and dichloromethane, yielded **17** and **18**, respec-

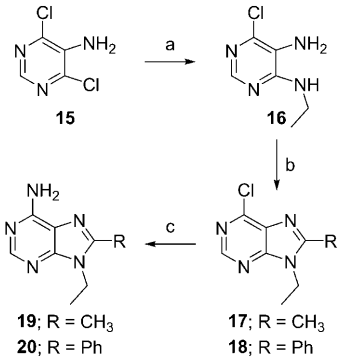

Scheme 3. Reagents and conditions: a) $EtNH_2$, 150 °C, 27 h; b) TEOA or TEOB, $MeSO_3H$; c) NH_3.

tively. These derivatives were successively treated with liquid ammonia, in sealed vials at room temperature, to obtain the desired 8-methyl- and 8-phenyladenine derivatives **19** and **20**.

Biology

All compounds were evaluated in binding assays using rat AA_1R, $AA_{2A}R$, and AA_3R. Displacement of [^{3}H]CHA (*N*6-cyclohexyladenosine) from AA_1R in rat cortical membranes and of [^{3}H]CGS 21680 (2-[4-(2-carboxyethyl)-phenethylamino]-5′-*N*-ethylcarboxamidoadenosine) from rat striatal membranes were performed as previously described.[29] The affinity for rat AA_3R was determined by displacement of [^{125}I]AB-MECA (*N*6-(3-iodo-4-aminobenzyl)-5′-*N*-methylcarboxamidoadenosine) in rat testis. Some of the compounds were also evaluated at human recombinant ARs that were transfected into Chinese hamster ovary (CHO) cells and analyzed with radioligand binding studies for AA_1R, $AA_{2A}R$, and AA_3R. Receptor binding affinity was determined using [^{3}H]CCPA (2-chloro-*N*6-cyclopentyladenosine) as the radioligand for AA_1R, whereas [^{3}H]NECA (5′-*N*-ethylcarboxamidoadenosine) was used for the $AA_{2A}R$ and AA_3R subtypes.[30] The data for rat and human receptors, reported as K_i or as percentage of inhibition at 10 or 20 μM, are listed in Tables 1 and 2.

Binding data analysis

Rat receptors

Most of the novel 8-substituted 9-ethyladenine derivatives demonstrated good affinity and selectivity for rat $AA_{2A}R$ (Table 1). Affinity for the AA_3R subtype was generally lower than for AA_1R, giving the compounds greater $AA_{2A}R/AA_3R$ selectivity as compared to $AA_{2A}R/AA_1R$ selectivity. In particular, the 8-halogen-substituted compounds (**2**–**4**) displayed affinity at rat $AA_{2A}R$ with K_i values in the high-nanomolar range and were slightly selective for the same receptor subtype (**2**: K_i $AA_{2A}R = 184$ nM; $AA_1R/AA_{2A}R = 2$, $AA_3R/AA_{2A}R > 109$; **3**: K_i $AA_{2A}R = 188$ nM; $AA_1R/AA_{2A}R > 106$, $AA_3R/AA_{2A}R > 106$; **4**: K_i $AA_{2A}R = 91$ nM; $AA_1R/AA_{2A}R = 8$, $AA_3R/AA_{2A}R = 19$); in fact, in some cases, the compounds did not bind either AA_1R or AA_3R when tested at concentrations as high as 10 or 20 μM. Replacement of the 8-halogen with a hydroxy group decreased the $AA_{2A}R$ binding affinity; however, the resulting compound (**5**; K_i $AA_{2A}R = 4037$ nM) retained $AA_{2A}R$ selectivity and did not bind either rat AA_1R or AA_3R.

Table 1. Affinities of 8-substituted-9-ethyladenines in radioligand binding assays at rat AA_1R, $AA_{2A}R$, and AA_3R.[a]

Compd	R	K_i [nM] AA_1R[b]	$AA_{2A}R$[c]	AA_3R[d]
2	Br	444 (394–446)	184 (169–199)	40 %[f]
3	Cl	30 %[f]	188 (166–211)	21 %[f]
4	I	699 (641–759)	91 (82–100)	1700 (1469–1946)
5	OH	30 %[e]	4037 (3982–4321)	7 %[e]
6	OCH_3	515 (465–563)	46 (39–50)	24 %[e]
7	OCH_2CH_3	4600 (4146–5076)	643 (565–726)	34 %[f]
8	$OCH(CH_3)_2$	615 (568–663)	$>10^5$	17000 (14908–19222)
9	$O(CH_2)_2$-cHex	12969 (11750–14244)	4400 (3839–4997)	7600 (6707–8546)
10	$O(CH_2)_2$-Ph	871 (824–918)	28 (24–33)	37 %[f]
11	furyl	40 (37–43)	153 (137–169)	900 (789–1018)
12	thiophenyl	45 (38–52)	208 (189–228)	0 %[f]
13	tetrahydrofuryl	33 %[e]	38 %[e]	14 %[e]
14	CF_3	982 (894–1023)	63 (57.6–65.8)	9 %[e]
19	CH_3	34 %[f]	2653 (2379–2650)	0 %[f]
20	Ph	11 (9.3–12)	763 (675–856)	1800 (1547–2070)

[a] 95 % confidence intervals of K_i values are given in parentheses. [b] Displacement of specific [^{3}H]CHA binding in rat cortical membranes, or percentage of specific binding inhibition. [c] Displacement of specific [^{3}H]CGS 21680 binding in rat striatal membranes, or percentage of specific binding inhibition. [d] Displacement of specific [^{125}I]AB-MECA binding in rat testis membranes, or percentage of specific binding inhibition. [e] Percent inhibition at 10 μM. [f] Percent inhibition at 20 μM.

Replacement of the 8-hydroxy group with alkoxy substituents (**6**–**10**) modulated the $AA_{2A}R$ binding affinity, indicative of different interactions with rat $AA_{2A}R$. The presence of small chains, such as methoxy or ethoxy, increased the $AA_{2A}R$ affinity (**6;** K_i $AA_{2A}R = 46$ nM and **7**; K_i $AA_{2A}R = 643$ nM), while the presence of an isopropoxy group was detrimental for affinity to $AA_{2A}R$ (**8;** K_i $AA_{2A}R > 100$ μM).

The presence of an aromatic and sterically hindered substituent, such as a phenethoxy group, at the 8-position highly favored the rat $AA_{2A}R$ interaction, yielding the most active compound of the entire series (**10**; K_i $AA_{2A}R = 28$ nM, selectivity: $AA_1R/AA_{2A}R = 31$, $AA_3R/AA_{2A}R > 714$). However, replacement of the phenyl ring found in **10** with a cyclohexyl substituent led to a remarkable decrease in $AA_{2A}R$ binding affinity (**9**; K_i $AA_{2A}R = 4400$ nM). The difference in $AA_{2A}R$ activity of compounds **9** and **10** may be attributed to different π-stacking in-

teractions of the compounds and contrasts in steric hindrance induced by the phenyl and cyclohexyl rings.

The presence of aromatic rings, such as furyl, thiophenyl, and phenyl, directly conjugated to the purine system was well tolerated by $AA_{2A}R$, but also favored interaction with the AA_1R subtype, as observed with **11**, **12** and **20**, which showed affinity for rat AA_1R in the nanomolar range and resulted in slightly AA_1R-selective profiles (**11;** K_i $AA_1R = 40$ nM; $AA_{2A}R/AA_1R = 4$, $AA_3R/AA_1R = 22$; **12**; K_i $AA_1R = 45$ nM; $AA_{2A}R/AA_1R = 5$, $AA_3R/AA_1R > 444$, and **20**; K_i $AA_1R = 11$ nM; $AA_{2A}R/AA_1R = 69$, $AA_3R/AA_1R = 164$). However, a lack of conjugation prevented interaction with all rat receptor subtypes, as evidenced by the binding data of **13** (inhibition at 10 μM of 33%, 38%, and 14% at rat AA_1R, $AA_{2A}R$, and AA_3R, respectively).

Finally, the 8-methyl derivative **19** exhibited moderate AA2AR affinity (K_i $AA_{2A}R = 2653$ nM) only twofold higher than that shown by the 8-hydroxy derivative **5**, but replacement with an 8-trifluoromethyl substituent yielded a considerable increase in $AA_{2A}R$ affinity (**14;** K_i $AA_{2A}R = 63$ nM). The differing affinities of these compounds might be explained by the abilities of the corresponding 8-substituents to polarize the aromatic adenine scaffold. This hypothesis is further supported by the $AA_{2A}R$ binding data obtained for compounds **2**–**4**, **6**, and **7**, which contain 8-halogen or 8-alkoxy substituents that have different polarizing effects.

Human receptors

The affinity of the 8-substituted 9-ethyladenine derivatives (compounds **2**, **7**–**11**, **14**, and **20**) was generally higher for human ARs than for rat receptors (Table 2). This finding, in agreement with our observations of a series of 2- and 8-alkynyl-9-ethyladenines previously reported,[17] might be explained by taking into account the differences in in vitro models of human and rat receptors. On the other hand, similar activity trends were observed for both receptor species, as most compounds were selective $AA_{2A}R$ antagonists in rat and human receptors. Accordingly, compound **8**, bearing an isopropoxy substituent, and compound **20**, bearing a phenyl ring directly conjugated to the purine scaffold, resulted in selective ligands for the AA_1R subtype at both rat and human receptors. The similarities in affinity for rat and human receptor subtypes does not hold true only for the conjugated 8-furyl derivative (compound **11**), which exhibited AA_1R selectivity for rat receptors ($AA_{2A}R/AA_1R = 4$) and $AA_{2A}R$ selectivity for human receptors ($AA_1R/AA_{2A}R = 6$). Notably, this compound was the most active $AA_{2A}R$ ligand among those tested in the human subtypes, followed by the 8-ethoxy and 8-bromo derivatives (compounds **7** and **2**) with K_i values of 46 and 52 nM, respectively.

Furthermore, as in the case of rat receptors, the affinity of the 8-substituted 9-ethyladenine derivatives for the human AA_3R subtype was generally lower than at AA_1R and $AA_{2A}R$, leading to compounds endowed with higher selectivity for the $AA_{2A}R$ versus the AA_3R, as compared to the AA_1R, subtypes.

Table 2. Affinities of 8-substituted-9-ethyladenines in radioligand binding assays at human AA_1R, $AA_{2A}R$, and AA_3R.[a]

Compd	R	K_i [nM]		
		AA_1R[b]	$AA_{2A}R$[c]	AA_3R[d]
2	Br	280 (250–320)	52 (24–110)	27800 (22300–34700)
7	OCH_2CH_3	2400 (2100–2600)	46 (24–91)	21000 (11000–41000)
8	$OCH(CH_3)_2$	440 (390–490)	$>10^5$	12000 (6000–22000)
9	$O(CH_2)_2$-*c*Hex	9000 (5600–14000)	2600 (2100–3100)	7500 (6800–8200)
10	$O(CH_2)_2$-Ph	890 (590–1330)	150 (96–230)	36200 (16900–77600)
11	furyl	24 (16–34)	3.7 (3.0–4.6)	4700 (2900–7600)
14	CF_3	631 (554–719)	80 (50–128)	20600 (19800–21500)
20	Ph	27 (15–47)	360 (140–980)	3300 (1500–7100)

[a] 95% confidence intervals of K_i values are given in parentheses. [b] Displacement of specific [^{3}H]CCPA binding in CHO cells, stably transfected with human recombinant AA_1R. [c] Displacement of specific [^{3}H]NECA binding in CHO cells, stably transfected with human recombinant $AA_{2A}R$. [d] Displacement of specific [^{3}H]NECA binding in CHO cells, stably transfected with human recombinant AA_3R.

Molecular modeling

A molecular docking analysis of the adenine derivatives was performed using a homology model of rat $AA_{2A}R$, which was built with the recently published human $AA_{2A}R$ crystal structure as a template,[27] with the ultimate aim at producing a possible rationalization for the different binding affinities of the molecules for rat $AA_{2A}R$. The human $AA_{2A}R$ crystal structure was solved in complex with ZM241385 antagonist, hence the template structure already contains a cavity suitable for a binding site. This is one of the most significant differences with respect to previously used templates, in particular the bovine rhodopsin crystal structures.

Another important feature of this crystal structure is the fold of the extracellular loop 2 (EL2) region, which is presented as a short α-helix segment in the human $AA_{2A}R$ structure, but as two β-strands in the bovine rhodopsin structures. Furthermore, the human $AA_{2A}R$ structure presents four disulfide bridges located in the extracellular loops, instead of the unique analogue feature present in the bovine rhodopsin crystal structures. The homology modeling of rat $AA_{2A}R$ was straightforward due to the high sequence similarity (approximately 82%) between rat and human receptors. The obtained model was subjected to stages of checking and refinement in order to verify and correct unwanted atom clashes or *cis*-amide peptide bonds. The obtained rat $AA_{2A}R$ model (Figure 1) was used as a target for the docking analysis of various adenine derivatives, and the obtained docking conformations were subjected to energy minimization. Due to the presence of water molecules in the template crystal structure which play a relevant role in the human $AA_{2A}R$–ZM241385 interaction, we chose to reintroduce these water molecules in the rat $AA_{2A}R$ binding site for post-docking energy minimization, in order to verify possible roles of solvent molecules in the stabilization of adenine binding

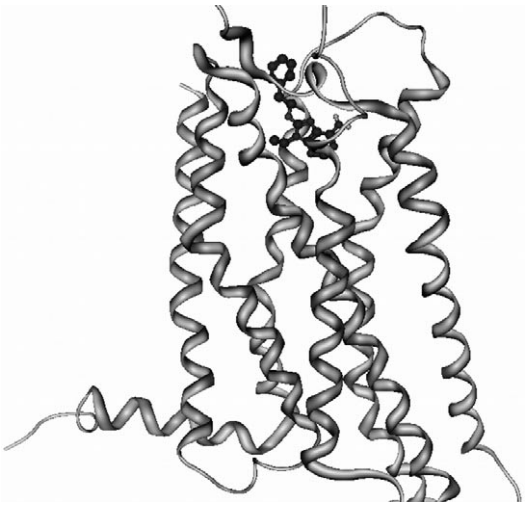

Figure 1. Homology model of rat $AA_{2A}R$. Docking conformation of compound **1** (ball-and-stick representation) indicates the location of the binding site.

and to compare these roles to those observed in the human $AA_{2A}R$-ZM241385 interaction. The binding cavity of rat $AA_{2A}R$ (Figure 2) was inserted between the TM2 (A60, I63) TM3 (A78, V81, L82, L84, T85), EL2 (F163, E164), TM5 (V173, N176, F177) TM6 (W241, L244, H245, N248), and TM7 (I269, S272, H273) domains.

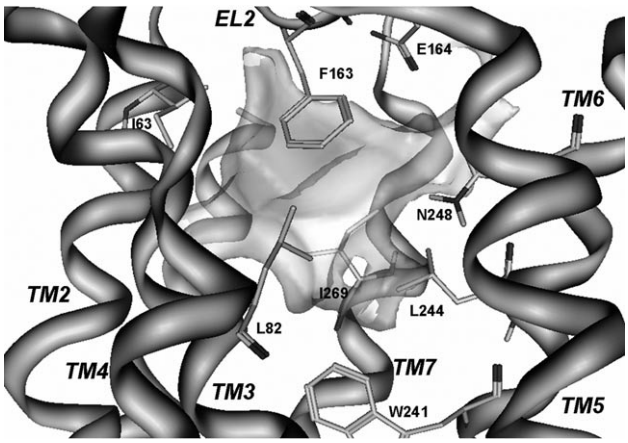

Figure 2. Binding cavity location and shape; residues involved in compound binding are indicated.

Our analyzed derivatives present several structural analogies with respect to the originally co-crystallized ZM241385 antagonist, which can be viewed as a "comparison term" in our analysis. Observing the general binding mode of the adenine derivatives, it was noted that the orientations of the bicyclic scaffold are grouped into two families. For the first family (Figure 3), docking simulation results for most of the derivatives share a similar binding motif inside the transmembrane (TM) region of rat $AA_{2A}R$, with the adenine pyrimidine ring located between TM3 and TM6 domains and the imidazole ring located between TM3 and TM7 helices. This scaffold orientation causes

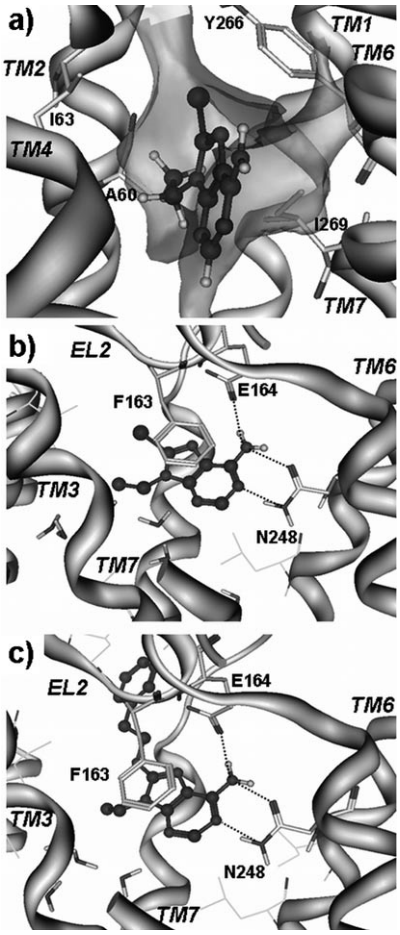

Figure 3. a) Top view of docking conformation for compound **4**; binding cavity volume is indicated by surface representation; TM2 and TM7 residues involved in the definition of the *N*9-ethyl and C8 substituent subpocket are indicated. Side views of docking conformations for b) compound **4** and c) compound **10**; residues with primary interactions are indicated; hydrogen bonds are represented as dashed lines.

the 8-position substituents to be oriented toward the top of the receptor, while the N1-C2-N3 region of the adenine scaffold projects toward the central TM core. Key receptor residues for the interaction with these derivatives are F163, E164 and N248, corresponding to human $AA_{2A}R$ F168, E169 and N253, respectively. The F163 phenyl ring and the adenine scaffold form a π–stacking interaction, while the E164 carboxy group and N248 amide functionalities are involved in hydrogen bonding with the N6 amine of the adenine core. Furthermore, the N248 amide gives an additional polar interaction with N1 of the adenine scaffold.

The 9-ethyl group and the 8-position substituent are located in a narrow subpocket between TM2 (A60 and I63) and TM7 (Y266 and I269). The shape and the volume of this subpocket allow the presence of only small groups in addition to the 9-ethyl substituent (Figure 3a). This may explain why halogens or other small substituents such as methyl, trifluoromethyl, methoxy, and ethoxy are well tolerated (Figure 3b) and at the same time could explain the inactivity of compound **8**, as it bears a more sterically hindered isopropoxy substituent at the 8-position. Compounds **9** and **10** (cyclohexylethoxy and phe-

nethoxy substituents, respectively) conformations belong in this family as well, and in this case the narrow subpocket is occupied by the ethoxy "spacer," while the six-membered rings are located externally with respect to the binding site (Figure 3c), analogously to the ZM241385 "tail" segment in the human $AA_{2A}R$ crystal structure. Finally, the 9-ethyl substituent is located in a position originally occupied by a water molecule in the human $AA_{2A}R$ crystal structure. During energy refinement of docking conformations, this water molecule was displaced from its original position and relocated to a position within proximity of N3 on the adenine scaffold.

The second family of docking conformations is presented by adenine derivatives substituted in the 8-position with various furyl, thiophenyl, and phenyl aromatic rings (compounds **11**, **12** and **20**, respectively). In this case, the binding motif is "inverted" with respect to the first family of docking conformations; the 8-substituent projects toward the central TM core. This scaffold orientation is similar to that observed for ZM241385, particularly for compound **11** (8-furyl substituent), which is located in the binding site in a nearly superimposable fashion relative to the analogous molecular area within the co-crystallized structure, presenting identical interactions with the receptor as observed with ZM241385 (Figure 4).

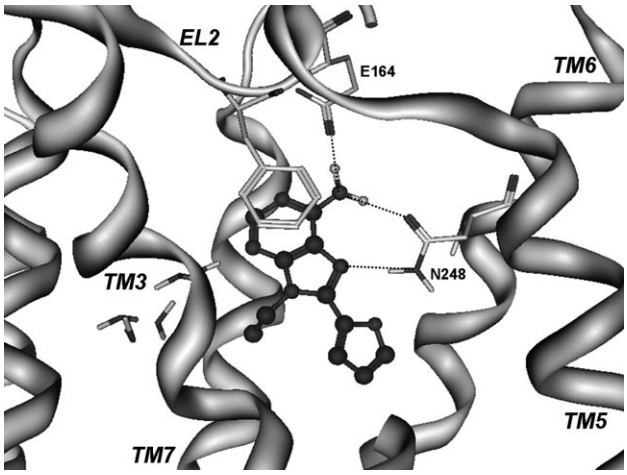

Figure 4. Side view of docking conformation for compound **11**; residues with primary interactions are indicated; hydrogen bonds are represented as dashed lines.

As seen in the co-crystal structure, the F163 phenyl ring and adenine scaffold form a π-stacking interaction, while the double hydrogen bonding interaction of the N248 amide group with the N6 amino group and N7 atom of adenine is analogous to the interaction of ZM241385 with N253 of human $AA_{2A}R$.[27] The aromatic substituent is located in a subpocket within proximity of L82, M172, L244, H245, and N248, and it presents partially hydrophobic and partially hydrophilic characteristics. This feature is the basis of the higher affinity observed for compound **11** relative to compounds **12** and **20**.

Additionally, the subpocket is partially filled by the 9-ethyl substituent, decreasing the available space for large 8-position substituents. As a consequence, the affinity is decreased when 8-substituent size increases (size: 8-furyl < 8-thiophenyl < 8-phenyl; K_i rat $AA_{2A}R$: 8-furyl < 8-thiophenyl < 8-phenyl), and when the aromatic furyl ring is fully reduced to the bulkier tetrahydrofuryl group, $AA_{2A}R$ affinity is lost. During energy refinement of docking conformations, the presence of the 9-ethyl substituent (not present in the corresponding position of the ZM241385 co-crystal structure) caused the water molecules to rearrange slightly, although they maintained their approximate original positions and orientations.

Very interestingly, by superimposing the docking conformations of compounds **10** and **11** (the compounds with the highest rat $AA_{2A}R$ affinity for each family of docking conformations) and comparing them with the binding mode of ZM241385 in the co-crystal structure (Figure 5), it is possible to note the interactions that are conserved for these compounds. Additionally, this superimposition enables evaluation of the substituent roles for the adenine derivatives, particularly the 9-ethyl group, which modulates the interaction with the receptor.

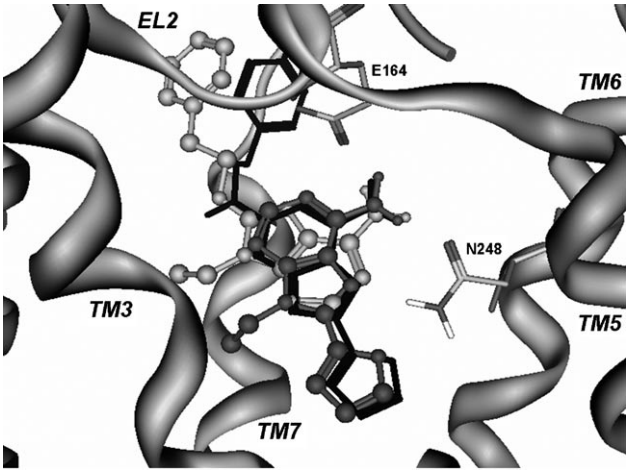

Figure 5. Superimposition of ZM241385 (black) in its original position and orientation in the human $AA_{2A}R$ crystal structure and the docking conformations for compounds **10** (light gray) and **11** (medium gray).

Other observations from this comparative method suggest that exploration of the 2-position of adenine derivatives may be beneficial, possibly in combination with 8-substitutions. In fact, compounds within the first family of docking conformations exhibit potential 2-substituents in the location occupied by the furyl substituent of ZM241385; alternatively, the orientation of compounds with "family 2" docking conformations suggests that a possible 2-substituent would instead correspond to the ZM241385 phenylethylamino chain. With regard to either of these hypotheses, a combination of 2- and 8-substituents could lead to more active compounds at $AA_{2A}R$.

Conclusions

Binding data for rat and human ARs demonstrated that the reported 8-substituted-9-ethyladenines behave as AR antagonists and that they are endowed, with few exceptions, of different degrees of selectivity for the $AA_{2A}R$ subtype. In addition, there

is a good correlation between affinity data for the two species. Notably, the three $AA_{2A}R$ antagonists **2**, **7**, and **11**, with a bromine, an ethoxy, and a furyl ring, respectively, in the 8-position of 9-ethyladenine not only exhibited excellent activity in the in vivo models of Parkinson's disease, but are the most active $AA_{2A}R$ antagonists for human receptors (**2**; K_i $hAA_{2A}R = 52$ nM; $rAA_{2A}R = 184$ nM; **7**; K_i $hAA_{2A}R = 46$ nM; $rAA_{2A}R = 643$ nM; **11**; $hAA_{2A}R = 3.7$ nM; K_i $rAA_{2A}R = 153$ nM). However, the newly synthesized 8-iodo, 8-methoxy, 8-phenethoxy, and 8-trifluoromethyl derivatives (**4**; K_i $AA_{2A}R = 91$ nM, **6**; K_i $AA_{2A}R = 46$ nM, **10**; K_i $AA_{2A}R = 28$ nM, and **14**; K_i $AA_{2A}R = 63$ nM, respectively) exhibited higher affinity and selectivity than observed for **2**, **7**, and **11** at rat $AA_{2A}R$. In particular, compound **10** had 28 nM affinity and 31-fold selectivity versus AA_1R, and may provide a new option suitable for in vivo studies in rat models of Parkinson's disease. Molecular modeling studies provided a description of two different potential binding modes of the synthesized ligands and their partially shared interactions with rat $AA_{2A}R$. Without a doubt, the recent crystallization of human $AA_{2A}R$ will have significant impact and utility for the analysis of purinergic receptor structures, the rationalization of different binding affinities of the corresponding ligands, and the design of new molecules with improved affinity and selectivity at human $AA_{2A}R$.

Experimental Section

Synthesis

General: Melting points were determined using a Büchi apparatus and are uncorrected. ^{1}H NMR spectra were obtained using a Mercury 400 MHz spectrometer; δ values in ppm, J values in Hz. All exchangeable protons were confirmed by addition of D_2O. Thin layer chromatography (TLC) was carried out on TLC plates with silica gel 60 F_{254} (Merck). For column chromatography, silica gel 60 (Merck) was used. Elemental analyses were determined using a Fisons Instruments Model EA 1108 CHNS-O model analyzer and are within ± 0.4% of theoretical values.

8-Chloro-9-ethyl-9*H*-adenine (3): NCS (163 mg, 1.22 mmol) was added to a solution of **1** (100 mg, 0.61 mmol) in dry DMF (10 mL), and the reaction mixture was stirred at room temperature for 20 h. The solvent was removed under vacuum, and the remaining residue was partitioned between H_2O and $CHCl_3$. The combined organic layers were washed with 2 N NaOH, dried over anhydrous Na_2SO_4, filtered, and concentrated under vacuum. The crude product was purified by preparative TLC, eluting with $CHCl_3$/*c*-hexane/MeOH (85:10:5) to obtain **3** (51 mg; 43% yield) as a white solid; mp: 218–220 °C (MeOH); ^{1}H NMR ([D$_6$]DMSO): $\delta = 1.34$ (t, 3H, J = 7.3 Hz, CH_3), 4.19 (q, 2H, $J = 7.2$ Hz, CH_2), 7.38 (s, 2H, NH_2), 8.17 ppm (s, 1H, H-2); Anal. ($C_7H_8ClN_5$) C, H, N.

9-Ethyl-8-iodo-9*H*-adenine (4): A solution of **1** (500 mg, 3.1 mmol) in dry THF (10 mL) was added dropwise to a solution of LDA (15.5 mmol) in dry THF (6 mL), maintained at −70 °C. After 1 h, a solution of I_2 (1.22 g, 4.9 mmol) in dry THF (10 mL) was added dropwise at −70 °C. After 1 h, the reaction was quenched by adding 4 drops of acetic acid and 3 mL MeOH. Volatile constituents were removed under vacuum, and the residue was purified by flash chromatography on a flash silica gel column with $CHCl_3$/MeOH (98:2) eluent to obtain **4** (570 mg, 64% yield) as a white powder; mp: 247–249 °C (MeOH); ^{1}H NMR ([D$_6$]DMSO): $\delta = 1.31$ (t, 3H, $J = 7.2$ Hz, CH_3), 4.12 (q, 2H, $J = 7.2$ Hz, CH_2), 7.34 (s, 2H, NH_2), 8.08 ppm (s, 1H, H-2); Anal. ($C_7H_8IN_5$) C, H, N.

9-Ethyl-8-hydroxy-9*H*-adenine (5): A solution of **2** (100 mg, 0.41 mmol) in 98% formic acid (10 mL) was stirred at reflux overnight. The formic acid was removed under vacuum, and the mixture was co-evaporated three times with H_2O. Compound **5** was obtained from crude residue via recrystallization from H_2O (86% yield); mp: 225–227 °C (H_2O); ^{1}H NMR (400 MHz, [D$_6$]DMSO): δ = 1.18 (t, 3H, $J = 7.0$ Hz, CH_3), 3.74 (q, 2H, $J = 7.0$ Hz, CH_2), 6.40 (br s, 2H, NH_2), 8.00 (s, 1H, H-2), 10.20 ppm (br s, 1H, OH); Anal. ($C_7H_9N_5O$) C, H, N.

9-Ethyl-8-methoxy-9*H*-adenine (6): A solution of **2** (400 mg, 1.65 mmol) and NaOH (5 mmol) in MeOH (20 mL) was stirred at 80 °C for 3 h. The solvent was removed under vacuum, and the residue was neutralized with 2 N HCl, then partitioned between H_2O and $CHCl_3$. The combined organic extracts were dried over anhydrous Na_2SO_4 and concentrated under vacuum. The residue was purified using a silica gel column, eluting with $CHCl_3$/*c*-hexane/MeOH (70:28:2) to obtain compound **6** (255 mg, 80% yield) as a white solid; mp: 177–179 °C; ^{1}H NMR ([D$_6$]DMSO): $\delta = 1.25$ (t, 3H, $J = 7.2$ Hz, NCH_2CH_3), 3.93 (q, 2H, $J = 7.2$ Hz, CH_2), 4.08 (s, 3H, OCH_3), 6.77 (br s, 2H, NH_2), 8.01 ppm (s, 1H, H-2); Anal. ($C_8H_{11}N_5O$) C, H, N.

8-Ethoxy-9-ethyl-9*H*-adenine (7): A solution of **2** (100 mg, 0.41 mmol) and NaOH (5 mmol) in EtOH (5 mL) was stirred at 80 °C for 16 h. The solvent was removed under vacuum, and the residue was neutralized with 2 N HCl, then partitioned between H_2O and $CHCl_3$. The combined organic extracts were dried over anhydrous Na_2SO_4 and concentrated under vacuum. The residue was purified using a silica gel column, eluting with $CHCl_3$/MeOH (95:5) to obtain compound **7** (66 mg, 80% yield), as a white solid; mp: 181–183 °C (MeOH); ^{1}H NMR ([D$_6$]DMSO): $\delta = 1.28$ (t, 3H, $J = 7.1$ Hz, NCH_2CH_3), 1.42 (t, 3H, $J = 7.1$ Hz, OCH_2CH_3), 3.96 (q, 2H, $J = 7.1$ Hz, NCH_2), 4.53 (q, 2H, $J = 7.1$ Hz, OCH_2), 6.78 (br s, 2H, NH_2); 8.04 ppm (s, 1H, H-2); Anal. ($C_9H_{13}N_5O$) C, H, N.

9-Ethyl-8-isopropoxy-9*H*-adenine (8): A solution of **2** (200 mg, 0.82 mmol) and NaOH (5 mmol) in *i*PrOH (10 mL) was stirred at 100 °C for 24 h. The solvent was removed under vacuum, and the residue was neutralized with 2 N HCl, then partitioned between H_2O and $CHCl_3$. The combined organic extracts were dried over anhydrous Na_2SO_4 and concentrated under vacuum. The residue was purified using a silica gel column, eluting with $CHCl_3$/MeOH (95:5) to obtain compound **8** (100 mg, 58% yield) as a white solid; mp: 112–115 °C; ^{1}H NMR ([D$_6$]DMSO): $\delta = 1.27$ (t, 2H, $J = 7.2$ Hz, NCH_2CH_3), 1.42 (d, 6H, $J = 6.1$ Hz, $OCH(CH_3)_2$), 3.95 (q, 2H, $J = 7.1$ Hz, NCH_2CH_3), 4.51 (t, 1H, $J = 6.6$ Hz, OCH_2), 6.76 (s, 2H, NH_2), 8.04 ppm (s, 1H, H-8); Anal. ($C_{10}H_{15}N_5O$) C, H, N.

8-(2-Cyclohexylethoxy)-9-ethyl-9*H*-adenine (9): A solution of **2** (200 mg, 0.83 mmol), NaOH (5.00 mmol), and cyclohexylethanol (0.84 mL; 6.08 mmol) in DMF (5 mL) was stirred at 80 °C for 8 h. The solvent was removed under vacuum, and the residue was neutralized with 2 N HCl, then partitioned between H_2O and $CHCl_3$. The combined organic extracts were dried over anhydrous Na_2SO_4 and concentrated under vacuum. The residue was purified using a silica gel column, eluting with $CHCl_3$/MeOH (98:2) to obtain compound **9** (137 mg, 55% yield) as a white solid; mp: 128–131 °C; ^{1}H NMR ([D$_6$]DMSO): $\delta = 0.99$ (m, 2H, H-*c*Hex), 1.20 (m, 2H, H-*c*Hex), 1.27 (t, 3H, $J = 7.2$ Hz, NCH_2CH_3), 1.45 (m, 1H, H-*c*Hex), 1.71 (m, 6H, H-*c*Hex), 3.95 (q, 2H, $J = 7.2$ Hz, NCH_2CH_3), 4.51 (t, 2H, $J = 6.6$ Hz,

OCH_2)), 6.76 (s, 2H, NH_2), 8.04 ppm (s, 1H, H-8); Anal. ($C_{15}H_{23}N_5O$) C, H, N.

9-Ethyl-8-(2-furyl)-9*H*-adenine (11): 2-(Tributylstannyl)furan (3.3 mL, 10.48 mmol) and bis(triphenylphosphine)palladium dichloride (85 mg, 0.12 mmol) were added to a solution of **2** (500 mg, 2.07 mmol) in anhydrous THF (10 mL). The mixture was held at reflux for 5 h, and was then concentrated under vacuum, and the residue was purified by preparative TLC using $CHCl_3$/MeOH (95:5) as eluent to obtain compound **11** (365 mg, 77% yield) as a white powder; mp: 231–233 °C; ^{1}H NMR ([D_6]DMSO): δ = 1.35 (t, 3H, J = 7.0 Hz, CH_3), 4.44 (q, 2H, J = 7.0 Hz, CH_2), 6.78 (m, 1H, H-furyl), 7.18 (d, 1H, J = 3.5 Hz, H-furyl), 7.37 (s, 2H, NH_2), 8.01 (s, 1H, H-furyl), 8.18 ppm (s, 1H, H-2); Anal. ($C_{11}H_{11}N_5O$) C, H, N.

9-Ethyl-8-(2-thienyl)-9*H*-adenine (12): 2-(Tributylstannyl)thiophene (1.0 mL, 3.17 mmol) and bis(triphenylphosphine)palladium dichloride (50 mg, 0.071 mmol) were added to a solution of **2** (150 mg, 0.62 mmol) in dry THF (10 mL). The mixture was held at reflux for 24 h, and was then concentrated under vacuum, and the residue was purified by silica gel chromatography, eluting with $CHCl_3$/EtOAc/MeOH (70:25:5) to obtain compound **12** (76 mg, 50% yield) as a white solid; mp: 208–210 °C; ^{1}H NMR ([D_6]DMSO): δ = 1.37 (t, 3H, J = 7.2 Hz, CH_3), 4.44 (q, 2H, J = 7.2 Hz, CH_2), 7.28 (m, 3H, H-thienyl and NH_2), 7.72 (d, 1H, J = 4.6 Hz, H-thienyl), 8.01 (d, 1H, J = 6.1 Hz, H-thienyl), 8.18 ppm (s, 1H, H-2); Anal. ($C_{11}H_{11}N_5S$) C, H, N, S.

9-Ethyl-8-(2-tetrahydrofuryl)-9*H*-adenine (13): Compound **5** (150 mg, 0.65 mmol) was dissolved in *i*PrOH (45 mL). PdO (150 mg) and concentrated HCl (0.5 mL) were added, and the mixture was placed under hydrogenation conditions (H_2, 13 atm) at 65 °C. After 9 h the reaction mixture was filtered through Celite, the solvent was removed, and the residue was purified using column chromatography, eluting with EtOAc/*c*-hexane/MeOH (60:33:7) to obtain compound **13** as a white solid (51 mg; 34% yield); mp: 132–134 °C (CH_3CN); ^{1}H NMR ([D_6]DMSO): δ = 1.35 (t, 3H, J = 7.2 Hz, CH_2CH_3), 1.95–2.31 (m, 3H, 1H di-CH_2-3′ and CH_2-4′), 2.50–2.75 (m, 1H, H-3′), 3.83 (m, 2H, CH_2-5′), 4.24 (q, 2H, J = 7.2 Hz, CH_2-H_3), 5.21 (t, 1H, J = 6.6 Hz, H-2′), 7.16 (s, 2H, NH_2), 8.13 ppm (s, 1H, H-2); Anal. ($C_{11}H_{15}N_5O$) C, H, N, S.

9-Ethyl-8-(trifluoromethyl)-9*H*-purin-6-amine (14): CF_3COONa (446 mg, 3.28 mmol) and CuI (311 mg, 1.64 mmol) were added to a solution of **2** (200 mg, 0.82 mmol) in NMP (7 mL); the mixture was stirred at 80 °C under N_2 atmosphere for 2.5 h. The reaction mixture was partitioned with Et_2O, then the Et_2O extract was dried over anhydrous Na_2SO_4, filtered, and concentrated under vacuum. The residue was purified using a silica gel column and $CHCl_3$/MeOH/methanolic NH_3 (98:1:1) eluent to obtain compound **14** (25 mg, 13% yield) as a vitreous solid. ^{1}H NMR ([D_6]DMSO): δ = 1.29 (t, 3H, J = 7.2 Hz, CH_3), 4.10 (q, 2H, J = 7.2 Hz, CH_2), 7.32 (br s, 2H, NH_2), 8.06 ppm (s, 1H, H-2); ^{13}C NMR ([D_6]DMSO): δ = 14.90 (CH_3), 38.33 (CH_2), 101.77 (CF_3), 121.40 (C5), 150.42 (C8), 152.56 (C3 and C4), 154.59 ppm (C6); Anal. ($C_8H_8F_3N_5$) C, H, N.

5-Amino-4-chloro-6-ethylaminopyrimidine (16): A solution of **15** (400 mg, 2.44 mmol), $EtNH_2$ (0.18 mL, 2.72 mmol), and 1 mL of Et_3N in EtOH (20 mL) was heated in a steel vial at 150 °C for 27 h. The reaction mixture was concentrated under vacuum, and the residue was purified by chromatography on a silica gel column, eluting with $CHCl_3$/MeOH (99.5:0.5) to obtain compound **16** (370 mg, 88%) as a yellow solid: mp: 142–144 °C; ^{1}H NMR ([D_6]DMSO): δ = 1.16 (t, 3H, J = 7.3 Hz, CH_3), 3.39 (m, 2H, CH_2), 5.01 (s, 2H, NH_2), 6.67 (br s, 1H, NH), 7.72 ppm (s, 1H, H-2); Anal. ($C_6H_9ClN_4$) C, H, N.

6-Chloro-9-ethyl-8-methyl-9*H*-purine (17): Triethylorthoacetate (240 mL, 1.32 mmol) and methanesulfonic acid (80 μL) were added to a solution of **16** (200 mg, 1.20 mmol) in 10 mL dry CH_2Cl_2. The mixture was stirred at room temperature overnight. The solvent was evaporated under vacuum, and the residue was held at reflux with 1 N HCl (10 mL) for 2 h. The mixture was then neutralized with a saturated solution of $NaHCO_3$ and extracted with $CHCl_3$. The extract was washed with H_2O, dried over anhydrous Na_2SO_4, filtered, and concentrated under vacuum to get the crude product, which was then purified by flash chromatography over silica gel, eluting with $CHCl_3$/MeOH (98:2) to obtain compound **17** (98 mg, 42% yield) as a white solid; mp: 71–72 °C; ^{1}H NMR ([D_6]DMSO): δ = 1.37 (t, 3H, J = 7.2 Hz, CH_2CH_3), 2.68 (s, 3H, CH_3), 4.29 (q, 2H, J = 7.2 Hz, CH_2CH_3), 8.71 ppm (s, 1H, H-2); Anal. ($C_8H_9ClN_4$) C, H, N.

6-Chloro-9-ethyl-8-phenyl-9*H*-purine (18): Triethylorthobenzoate (147 μL, 0.65 mmol) and methanesulfonic acid (40 μL) were added to a solution of **16** (100 mg, 0.58 mmol) in CH_2Cl_2 (10 mL). The mixture was stirred at room temperature overnight. The solvent was removed under vacuum, and the residue was held at reflux for 2 h with 1 N HCl (5 mL). The reaction mixture was neutralized with a saturated solution of $NaHCO_3$ and then extracted with $CHCl_3$. The combined organic extracts were washed with H_2O, dried over anhydrous Na_2SO_4, filtered, and concentrated under vacuum to get the crude product, which was purified using preparative TLC with $CHCl_3$/MeOH (99:1) as eluent to obtain compound **18** (95 mg, 42% yield) as pure product; mp: 127–128 °C; ^{1}H NMR ([D_6]DMSO): δ = 1.38 (t, J = 7.0 Hz, 3H, CH_3), 4.42 (q, 2H, J = 7.2 Hz, CH_2), 7.67 (m, 3H, H-Ph), 7.90 (m, 2H, H-Ph), 8.83 ppm (s, 1H, H-2); Anal. ($C_{13}H_{11}ClN_4$) C, H, N.

9-Ethyl-8-methyl-9*H*-adenine (19): A solution of **17** (80 mg, 0.41 mmol) and NH_3(l) (10 mL) was sealed in a stainless steel tube and allowed to sit at room temperature for 24 h. The NH_3 was evaporated, and the residue was purified using preparative TLC, eluting with $CHCl_3$/MeOH (96:4) to obtain compound **19** (64 mg, 93% yield) as a white solid; mp: 222–224 °C; ^{1}H NMR ([D_6]DMSO): δ = 1.37 (t, 3H, J = 7.3 Hz, CH_2CH_3), 2.54 (s, 3H, CH_3), 4.15 (q, 2H, J = 7.3 Hz, CH_2CH_3), 7.03 (S, 2H, NH_2), 8.10 ppm (s, 1H, H-2); Anal. ($C_8H_{11}N_5$) C, H, N.

9-Ethyl-8-phenyl-9*H*-adenine (20): A mixture of **18** (40 mg, 0.16 mmol) and NH_3(l) (5 mL) was sealed in a stainless steel tube and allowed to sit at room temperature for 24 h. The NH_3 was evaporated, and the residue was purified using preparative TLC, eluting with $CHCl_3$/MeOH (98:2) to obtain 28 mg (75%) of compound **20** as a solid; mp: 183–185 °C; ^{1}H NMR ([D_6]DMSO): δ = 30 (t, 3H, J = 7.0 Hz, CH_2CH_3), 4.27 (q, 2H, J = 7.2 Hz, CH_2CH_3), 7.29 (S, 2H, NH_2), 7.60 (m, 3H, H-Ph), 7.78 (m, 2H, H-Ph), 8.20 ppm (s, 1H, H-2); Anal. ($C_{13}H_{13}N_5$) C, H, N.

Biology

Binding studies at rat ARs: AA_1R and $AA_{2A}R$ binding: displacement of [^{3}H]CHA (31 Ci mmol^{-1}) from AA_1R in rat cortical membranes and of [^{3}H]CGS 21680 (42.1 Ci mmol^{-1}) from rat striatal membranes were performed as previously described.[29] [^{125}I]AB-MECA binding to AA_3R of rat testis membranes was performed in 50 mM Tris, 10 mM $MgCl_2$, and 1 mM EDTA buffer (pH 7.4), containing 0.2 mg proteins and 25 nM DPCPX, to selectively block AA_1R subtypes. Incubations were carried out for 90 min at 25 °C. Nonspecific binding was determined in the presence of 50 μM R-PIA and accounted for 30% of total binding. The binding reactions were terminated by rapid filtration through a Whatman GF/C filter, washing with ice-cold buffer (3×5 mL). All compounds were routinely dissolved in DMSO

and diluted with assay buffer to the final concentration, with the amount of DMSO never in excess of 2%. At least six different concentrations of each compound were used, and IC_{50} values were computer-generated using a program incorporating a nonlinear regression formula (GraphPad Software, La Jolla, CA, USA). IC_{50} values were converted into K_i values by using known dissociation constant (K_d) values for the radioligands in the different tissues and following the Cheng–Prusoff equation.[31] The K_d values of [^{3}H]CHA, [^{3}H]CGS 21680, and [^{125}I]AB-MECA were 1.2, 10, and 1.35 nM, respectively.

Binding studies and adenylyl cyclase activity at human ARs: The radioligand binding experiments were performed as previously described.[30] For AA_1R binding, 1 nM [^{3}H]CCPA was used as a radioligand, whereas 30 and 10 nM [^{3}H]NECA was used for $AA_{2A}R$ and AA_3R, respectively. Nonspecific binding was determined in the presence of 1 mM theophylline (AA_1R) or 100 μM R-PIA ($AA_{2A}R$ and AA_3R). K_i values were calculated from competition curves by nonlinear curve fitting using the program SCTFIT.[32] CHO cells stably transfected with human adenosine receptors were grown adherently and maintained in Dulbecco's modified Eagle's medium with nutrient mixture F12 (DMEM/F12) without nucleosides, containing 10% fetal calf serum, penicillin (100 U mL^{-1}), streptomycin (100 μg mL^{-1}), L-glutamine (2 mM), and Geneticin (G-418, 0.2 mg mL^{-1}) at 37 °C in 5% CO_2/95% air as previously described.[30] For radioligand binding studies and measurement of adenylyl cyclase activity, crude membrane fractions were prepared from fresh or frozen cells with two different protocols which were described recently.[30] Determination of adenylyl cyclase activity also followed the procedure described.[30] IC_{50} values for inhibition of cyclase stimulated with 5 μM NECA were calculated using the Hill equation and were converted into K_i values using the Cheng–Prusoff equation. The Hill slopes were near unity, suggesting a competitive interaction for the antagonists tested.

Molecular modeling

Computational methodologies: All molecular modeling studies were performed on a two-CPU (PIV 2.0–3.0 GHz) Linux PC. Homology modeling and docking studies were carried out using the Molecular Operating Environment (MOE, version 2008.10) suite.[33] All ligand structures were optimized using RHF/AM1 semiempirical calculations, using the software package MOPAC implemented in MOE.[34]

Homology model of the rat $AA_{2A}R$: A homology model of the rat $AA_{2A}R$ was built using the recently solved X-ray crystal structure of the human $AA_{2A}R$ in complex with ZM241385 (PDB code: 3EML,[27] available at the RCSB Protein Data Bank, 2.6 Å resolution) as a template. The amino acid sequences of the TM helices in rat and human $AA_{2A}R$s were easily aligned, as they present approximately 82% sequence identity. The boundaries identified from the X-ray crystal structure of human $AA_{2A}R$ were applied for the corresponding sequences of the TM helices of rat $AA_{2A}R$. The loop domains of rat $AA_{2A}R$ were built by the loop search method implemented in MOE. Once the heavy atoms were modeled, all hydrogen atoms were added, and the protein coordinates were then minimized by MOE using the AMBER99 force field.[35] The minimizations were performed by 1000 steps of steepest descent, followed by conjugate gradient minimization, until the RMS gradient of the potential energy was less than 0.05 kJ mol^{-1} Å^{-1}.

Molecular docking of the rat $AA_{2A}R$ antagonists: The human $AA_{2A}R$ crystal structure was solved in complex with ZM241385 antagonist. The ligand was removed prior to receptor modeling, and the cavity occupied by this molecule, and still present in the obtained rat $AA_{2A}R$ model, was employed as the binding site region for the docking analyses. All antagonist structures were then docked using the MOE Dock tool, a method which is divided into a number of stages. First, for conformational analysis of ligands, the algorithm generated conformations from a single 3D conformation by conducting a systematic search. In this way, all combinations of angles were created for each ligand. For placement, a collection of poses was generated from the pool of ligand conformations using the Alpha Triangle placement method. Poses were generated by superimposing ligand atom triplets and triplet points in the receptor binding site. The receptor site points are alpha sphere centers which represent locations of tight packing. For each iteration, a random conformation was selected, and random triplets of ligand atoms and alpha sphere centers were used to determine the pose. Poses generated by the placement methodology were scored using two available methods implemented in MOE, the London dG scoring function which estimates the free energy of binding of the ligand from a given pose, and Affinity dG Scoring, which estimates the enthalpic contribution to the free energy of binding. The top-30 poses for each ligand were sent to a MOE database. Each resulting ligand pose was then subjected to MMFF94[36–42] energy minimization until the RMS gradient of the potential energy was less than 0.05 kJ mol^{-1} Å^{-1}. In this phase, water molecules originally present in the human $AA_{2A}R$ were recovered and subjected to energy minimization along with the ligands. AMBER99 partial charges of receptor and water molecules and MOPAC output partial charges of ligands were used.

Acknowledgements

The work was supported by a grant of the Italian Ministry for University and Research (PRIN2006, FIRB RBN503YA3L project).

Keywords: adenosine · antagonists · molecular modeling · purine derivatives · receptors

[1] K. A. Jacobson, Z. G. Gao, *Nat. Rev. Drug Discovery* **2006**, *5*, 247–264.
[2] G. Cristalli, R. Volpini, *Curr. Top. Med. Chem.* **2003**, *3*, 355–469.
[3] A. S. Robeva, R. L. Woodard, X. Jin, Z. Gao, S. Bhattacharya, H. E. Taylor, D. L. Rosin, J. Linden, *Drug Dev. Res.* **1996**, *39*, 243–252.
[4] B. B. Fredholm, A. P. IJzerman, K. A. Jacobson, K.-N. Klotz, J. Linden, *Pharmacol. Rev.* **2001**, *53*, 527–552.
[5] B. B. Fredholm, *Cell Death Differ.* **2007**, *14*, 1315–1323.
[6] M. A. Jacobson, *Expert Opin. Ther. Pat.* **2002**, *12*, 489–501.
[7] K.-N. Klotz, *Naunyn-Schmiedeberg's Arch. Pharmacol.* **2000**, *362*, 382–391.
[8] C. E. Muller, B. Stein, *Curr. Pharm. Des.* **1996**, *2*, 501–530.
[9] S. A. Poulsen, R. J. Quinn, *Bioorg. Med. Chem.* **1998**, *6*, 619–641.
[10] S. Hess, *Expert Opin. Ther. Pat.* **2001**, *11*, 1533–1561.
[11] P. G. Baraldi, M. A. Tabrizi, S. Gessi, P. A. Borea, *Chem. Rev.* **2008**, *108*, 238–263.
[12] J. P. van Veldhoven, L. C. Chang, J. K. von Frijtag Drabbe Kunzel, T. Mulder-Krieger, R. Struensee-Link, M. W. Beukers, J. Brussee, A. P. IJzerman, *Bioorg. Med. Chem.* **2008**, *16*, 2741–2752.
[13] G. Cristalli, E. Camaioni, S. Costanzi, S. Vittori, R. Volpini, K.-N. Klotz, *Drug Dev. Res.* **1998**, *45*, 176–181.
[14] E. Camaioni, S. Costanzi, S. Vittori, R. Volpini, K.-N. Klotz, G. Cristalli, *Bioorg. Med. Chem.* **1998**, *6*, 523–533.
[15] K.-N. Klotz, S. Kachler, C. Lambertucci, S. Vittori, R. Volpini, G. Cristalli, *Naunyn-Schmiedeberg's Arch. Pharmacol.* **2003**, *367*, 629–634.
[16] R. Volpini, S. Costanzi, S. Vittori, G. Cristalli, K.-N. Klotz, *Curr. Top. Med. Chem.* **2003**, *3*, 427–443.

[17] R. Volpini, S. Costanzi, C. Lambertucci, S. Vittori, C. Martini, M. L. Trincavelli, K.-N. Klotz, G. Cristalli, *Purinergic Signalling* **2005**, *1*, 173–181.
[18] H. Harada, O. Asano, Y. Hoshino, S. Yoshikawa, M. Matsukura, Y. Kabasawa, J. Niijima, Y. Kotake, N. Watanabe, T. Kawata, T. Inoue, T. Horizoe, N. Yasuda, H. Minami, K. Nagata, M. Murakami, J. Nagaoka, S. Kobayashi, I. Tanaka, S. Abe, *J. Med. Chem.* **2001**, *44*, 170–179.
[19] R. A. de Ligt, P. A. van der Klein, J. K. von Frijtag Drabbe Kunzel, A. Lorenzen, F. Ait El Maate, S. Fujikawa, R. van Westhoven, T. van den Hoven, J. Brussee, A. P. IJzerman, *Bioorg. Med. Chem.* **2004**, *12*, 139–149.
[20] M. Perreira, J. K. Jiang, A. M. Klutz, Z. G. Gao, A. Shainberg, C. Lu, C. J. Thomas, K. A. Jacobson, *J. Med. Chem.* **2005**, *48*, 4910–4918.
[21] B. B. Fredholm, Y. Chern, R. Franco, M. Sitkovsky, *Prog. Neurobiol.* **2007**, *83*, 263–276.
[22] K. Xu, E. Bastia, M. Schwarzschild, *Pharmacol. Ther.* **2005**, *105*, 267–310.
[23] N. Simola, M. Morelli, A. Pinna, *Curr. Pharm. Des.* **2008**, *14*, 1475–1489.
[24] G. Cristalli, B. Cacciari, D. Dal Ben, C. Lambertucci, S. Moro, G. Spalluto, R. Volpini, *ChemMedChem* **2007**, *2*, 260–281.
[25] G. Cristalli, C. Lambertucci, G. Marucci, R. Volpini, D. Dal Ben, *Curr. Pharm. Des.* **2008**, *14*, 1525–1552.
[26] A. Pinna, R. Volpini, G. Cristalli, M. Morelli, *Eur. J. Pharmacol.* **2005**, *512*, 157–164.
[27] V. P. Jaakola, M. T. Griffith, M. A. Hanson, V. Cherezov, E. Y. Chien, J. R. Lane, A. P. IJzerman, R. C. Stevens, *Science* **2008**, *322*, 1211–1217.
[28] P. G. Baraldi, A. U. Broceta, M. J. P. de Las Infantas, J. J. D. Mochun, A. Espinosa, R. Romagnoli, *Tetrahedron* **2002**, *58*, 7607–7611.
[29] V. Colotta, D. Catarzi, F. Varano, L. Cecchi, G. Filacchioni, C. Martini, L. Trincavelli, A. Lucacchini, *J. Med. Chem.* **2000**, *43*, 1158–1164.
[30] K.-N. Klotz, J. Hessling, J. Hegler, C. Owman, B. Kull, B. B. Fredholm, M. J. Lohse, *Naunyn-Schmiedeberg's Arch. Pharmacol.* **1998**, *357*, 1–9.
[31] Y. Cheng, W. H. Prusoff, *Biochem. Pharmacol.* **1973**, *22*, 3099–3108.
[32] A. De Lean, A. A. Hancock, R. J. Lefkowitz, *Mol. Pharmacol.* **1982**, *21*, 5–16.
[33] *Molecular Operating Environment*, CCG Inc., 1255 University St., Suite 1600, Montreal, QC, H3B 3X3 (Canada).
[34] J. J. Stewart, *J. Comput.-Aided Mol. Des.* **1990**, *4*, 1–105.
[35] W. D. Cornell, P. Cieplak, C. I. Bayly, I. R. Gould, K. M. Merz, D. M. Ferguson, D. C. Spellmeyer, T. Fox, J. W. Caldwell, P. A. Kollman, *J. Am. Chem. Soc.* **1995**, *117*, 5179–5197.
[36] T. A. Halgren, *J. Comput. Chem.* **1996**, *17*, 490–519.
[37] T. A. Halgren, *J. Comput. Chem.* **1996**, *17*, 520–552.
[38] T. A. Halgren, *J. Comput. Chem.* **1996**, *17*, 553–586.
[39] T. A. Halgren, *J. Comput. Chem.* **1996**, *17*, 587–615.
[40] T. A. Halgren, R. Nachbar, *J. Comput. Chem.* **1996**, *17*, 616–641.
[41] T. A. Halgren, *J. Comput. Chem.* **1999**, *20*, 720–729.
[42] T. A. Halgren, *J. Comput. Chem.* **1999**, *20*, 730–748.

Received: December 15, 2008
Revised: February 20, 2009
Published online on ■■ ▮▮, 2009

A new series of 8-substituted 9-ethyladenine derivatives has been synthesized and tested at rat and human adenosine receptors. Binding data demonstrates that some compounds could represent new tools suitable for in vivo studies in rat models of Parkinson's disease and for the design of new molecules with improved affinity and selectivity at human $AA_{2A}R$.

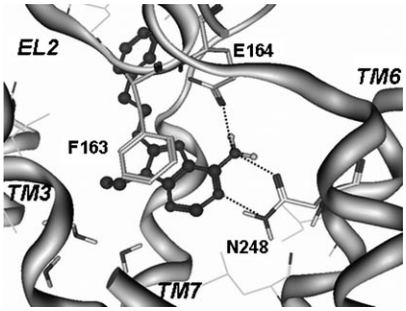

R. Volpini, D. Dal Ben, C. Lambertucci, G. Marucci, R. C. Mishra, A. T. Ramadori, K.-N. Klotz, M. L. Trincavelli, C. Martini, G. Cristalli*

■■ – ■■

Adenosine A_{2A} Receptor Antagonists: New 8-Substituted 9-Ethyladenines as Tools for in vivo Rat Models of Parkinson's Disease

